THE ASTROPHYSICAL JOURNAL, 327:870–875, 1988 April 15

HIGH SPATIAL RESOLUTION INFRARED IMAGING OF L1551–IRS 5: DIRECT OBSERVATIONS OF ITS CIRCUMSTELLAR ENVELOPE

ANDREA MONETI,[1,2] WILLIAM J. FORREST,[2] JUDITH L. PIPHER,[2] AND CHARLES E. WOODWARD[2,3]
University of Rochester, and C. E. K. Mees Observatory
Received 1987 March 16; accepted 1987 October 6

ABSTRACT

We have obtained images of L1551–IRS 5 at 1.65, 2.2, and 3.8 μm using the University of Rochester's Infrared Array Camera. We find that IRS 5 is spatially resolved, and that it is elongated: the observed FWHM size of IRS 5 is 4.1×2.8 arcsec^2 at 2.2 μm. These observations are interpreted in terms of a flattened circumstellar envelope that is viewed from about 18° above its equatorial plane, a configuration that has been treated theoretically by Lefèvre *et al.* In this model the central star is not seen directly, but only light scattered toward the observer from the visible polar region, where the envelope is thinnest, is observed. We deduce that the envelope has a diameter of 1000 AU, a molecular hydrogen density of greater than or approximately equal to 4×10^6 cm^{-3}, and a mass of greater than or approximately equal to 0.02 $M_\odot$, which results in an extinction of $A_V \gtrsim 33$ mag to the central source.

The direction of elongation is $\sim 135°$ which is roughly parallel to the position angle of the infrared polarization and perpendicular to the CO outflow and to the optical jet associated with IRS 5. This is discussed, and our model also explains qualitatively the large infrared polarization.

Subject headings: infrared: sources — stars: circumstellar shells; pre-main sequence

I. INTRODUCTION

The source IRS 5 in L1551 was discovered in a near-infrared survey of the L1551 dark cloud (Strom, Strom, and Vrba 1976). Subsequent observations have shown that the spectrum of IRS 5 peaks at about 100 μm, and that its bolometric luminosity is about 35 $L_\odot$ (Davidson and Jaffe 1984; Emerson *et al.* 1984, and references therein). The nature of IRS 5 is reviewed in Strom *et al.* (1985; henceforth SSGCT). The general concensus is that IRS 5 is a highly obscured young stellar object which is interacting with its environment. Snell, Loren, and Plambeck (1980, henceforth SLP) discovered an outflow of high-velocity molecular gas (namely CO) extending over 20′ into two streams on opposite sides of the IRS 5 (see also Snell and Schloerb 1984; Mirabel *et al.* 1985; Moriarty-Schieven *et al.* 1987). Within the blue-shifted stream are the Herbig-Haro (HH) objects HH-28 and HH-29 which have large proper motions indicating that they are moving away from a point near IRS 5 (Cudworth and Herbig 1979). Deep CCD images of IRS 5 and its surroundings (Mundt and Fried 1983; Snell *et al.* 1985) reveal several aligned knots of emission extending about 10″ away from IRS 5 toward the SW; these knots make up the optical jet. Farther to the SW is a large region of extended faint nebulosity (HH-102). The emission there has been shown to be light from IRS 5 scattered toward the observer (Draper, Warren-Smith, and Scarrot 1985; Nagata *et al.* 1986). IRS 5 has also been observed with the VLA at several frequencies (Rodríguez *et al.* 1986, and references therein). The 15 GHz structure of IRS 5 is interpreted as emission from the ionized inner part of a confining torus with radius of ~ 25 AU seen in projection plus extended emission from ionized gas accelerated by the wind (Rodríguez *et al.* 1986).

The L1551 cloud is permeated by a magnetic field oriented at a P.A. of $\sim 70°$ (Vrba, Strom, and Strom 1976) which, as noted by SLP, is about the same as the direction of the CO outflows. The distance to IRS 5 is about 150 pc (Elias 1978).

IRS 5 is very highly polarized (24% at 2.2 μm, Nagata, Sato, and Kobayashi 1983; Hodapp 1984), with the position angle of the polarization (P.A. $\approx 160°$) nearly perpendicular to the direction of the outflow and of the optical jet. Nagata, Sato, and Kobayashi (1983) interpreted the polarization in terms of the model of Elsässer and Staude (1978, henceforth ES), i.e., in terms of large-scale scattering from a bipolar nebula around the source. Furthermore, multiaperture polarimetry (Hodapp 1984) shows that the polarization does not change with beam size (for beam sizes greater than 4″). These results suggest that the scattering lobes must be present within a 4″ beam centered on the source. If the interpretation in terms of the ES model is correct, the scattering lobes could be visible on near-infrared images of IRS 5, and if they are small, they may appear as an extension of the source in a direction perpendicular to the polarization.

In order to investigate IRS 5 and its environs, we obtained infrared images of IRS 5 with 1″ spatial resolution using the University of Rochester's Infrared Array Camera (Forrest *et al.* 1985; Moneti 1984). The observational techniques and the results are presented in § II. Our observations show that IRS 5 is indeed extended but that the extension is perpendicular to the direction expected on the basis of the ES model. This result is interpreted in terms of a central star with a flattened circumstellar envelope that is viewed nearly edge-on; the model is presented and discussed in § III. The results are summarized in § IV. A preliminary version of these results was present in Moneti *et al.* (1986).

SSGCT have also presented 2.2 μm images of IRS 5 which they obtained using a different technique. Those images are similar to the one presented here, though some important differences will be noted. Finally, our interpretation is an alternative to that of SSGCT.

[1] Now at European Southern Observatory.

[2] Visiting Astronomer at Kitt Peak National Observatory, National Optical Astronomy Observatories, which is owned and operated by the Association of Universities for Research in Astronomy, Inc., under contract with the National Science Foundation.

[3] Now at the Wyoming Infrared Observatory.

II. OBSERVATIONS AND DATA ANALYSIS

The observations presented here were obtained on 1984 January 26 using the University of Rochester's Infrared Array Camera mounted on the NOAO-Kitt Peak 1.3 m telescope. The array camera and the observing and data processing techniques have been described in Forrest *et al.* (1985) and in Moneti (1984). In brief, the instrument uses a 32 × 32 element array of indium antimonide detectors that is bump-bonded to a silicon CCD which is used for charge storage and read-out. IRS 5 was observed through H ($\langle\lambda\rangle = 1.65$ μm, $\Delta\lambda = 0.32$ μm), K ($\langle\lambda\rangle = 2.23$ μm, $\Delta\lambda = 0.41$ μm), and L' ($\langle\lambda\rangle = 3.75$ μm, $\Delta\lambda = 0.81$ μm) filters. Several images of the source were obtained at each wavelength, and after every two images a piece of blank sky near the source was observed. We did not use the telescope's chopping secondary to rapidly alternate between source and sky, thus avoiding possible problems arising from inaccuracies in the motion of the secondary. As part of the data processing, the sky frames (actually, a linear combination of the sky before and the sky after) were subtracted from data frames, and the resulting frames were flat-fielded. Finally, these images were positionally justified and co-added to produce the pictures shown in Figures 1 and 2 (Plates 8 and 9). The final resolution of the system, when mounted on the 1.3 m telescope, is 0".976, 0".967, and 0".990 per pixel at H, K, and L', respectively, and the total field of view is about 31 × 31 arcsec^2. In Figure 1 the gray levels are scaled linearly, and in Figure 2 they are scaled logarithmically in order to emphasize the regions of low surface brightness. For comparison, we have obtained images of two point sources (α Ari and α CMi) before and after the observations of IRS 5. An image of α Ari at K is presented in the figures. The results are also shown as contour plots in Figure 3. The integration times on IRS 5 were 18, 13, and 6 minutes in H, K, and L', respectively. The width of the images of the point sources was about 1".7.

a) Description of the Images

The images in Figure 1 clearly reveal the extended nature of IRS 5. These images, being linearly scaled, show roughly the full width at half-maximum (FWHM) size of IRS 5 and of the comparison star, and they also clearly show that IRS 5 is elongated along an axis at ~135°. The elongation is particularly notable in the K and L' images. The contour plots, in which the contour levels are logarithmic (see caption to Fig. 3 for details), also show that some coma is present in the image of the comparison star, and that the coma extends toward the NE, perpendicular to the direction of the extension of IRS 5. We will discuss the extended nature of IRS 5 quantitatively in the next paragraph.

The H image shows several low-level protrusions that appear to be related to features in the i band (~0.9 μm) image obtained by B. Campbell (private communication). In particular, there are two parallel jet-like features at a position angle of 250°; these features are about 5" long and unresolved in width, they are separated by ~4", and the northern one is weaker than the southern one. Other knots of emission are present south of the main source, and our images do not extend far enough to the west, beyond the optical jet, where several optical knots are located (Mundt and Fried 1983). We also find that the H band emission falls off much more steeply on the NE side of the peak than on the SW side.

In the K image there are weak features that are reminiscent of the H protrusions. The most prominent feature at K, however, is a region of faint emission that extends southward almost to the bottom of the frame; this emission is roughly spatially coincident with the southern knots observed at H, though the K emission there is less knotty in appearance. We will henceforth refer to the southern extension as the arc. When the lowest signal levels in the K data are emphasized, there is a low signal-to-noise suggestion that another arclike structure may be present to the NW, but deeper images are needed to confirm this. In the L' image, where the sky noise is rather high, the extended nature of IRS 5 is evident, but neither the arc nor any of the protrusions are detected there.

SSGCT used a single element detector to obtain highly oversampled K images which were then processed using a "maximum entropy" technique to increase the spatial resolution. There are two ways in which our K image differs from those of SSGCT: first, our image does not show the cusp-shaped structure found by SSGCT, and second, considerable elongation is seen even in our highest contours, while in the images of SSGCT the highest contours are fairly round. The elongation of the high level contours is observed in our data also at H and especially at L'.

b) Image Measurements

In order to correctly interpret the features seen in the images, one must attempt to remove structure that is introduced by the imperfect imaging qualities of the telescope and of dewar optics. The point spread function of the system (or beam) was obtained from images of point sources obtained at various wavelengths before and after the images of IRS 5. Visual inspection of the beam showed that it was slightly elongated with the major axis at a position angle of approximately 135°. Cuts through the centroid of the light distribution of the point source images were obtained and measured, and the mean beam size was 1.9 × 1.6 arcsec^2 (FWHM) measured along the 135° and the 45° axes (i.e., the major and minor axes), respectively, with an uncertainty of 0".1 in both directions. No significant variation in beam size or shape was found either with wavelength or with time.

The sizes of IRS 5 at the different passbands, measured both parallel and perpendicular to a 135° axis, together with the eccentricities e of the images are presented in Table 1. For comparison, the eccentricity of the beam was 0.29. The last three columns of Table 1 list the sizes and the eccentricities of the IRS 5 images after the beam was subtracted in quadrature. These results confirm what was determined visually from Figures 1 and 2.

c) Flux Calibration

Photometric standard stars were observed for flux calibration. The signal from a star is given by the sum of the signals in each detector illuminated by the star. In practice the

TABLE 1

WIDTH OF SOURCE IMAGES[a]

	Raw Data			Corrected Data[b]		
Filter	a	b	e	a	b	e
H	4.2	3.7	0.22	3.8	3.3	0.35
K	4.1	2.8	0.53	3.6	2.3	0.59
L'	4.6	3.3	0.49	4.2	2.9	0.52

[a] In seconds of arc.
[b] With the beam size subtracted in quadrature.

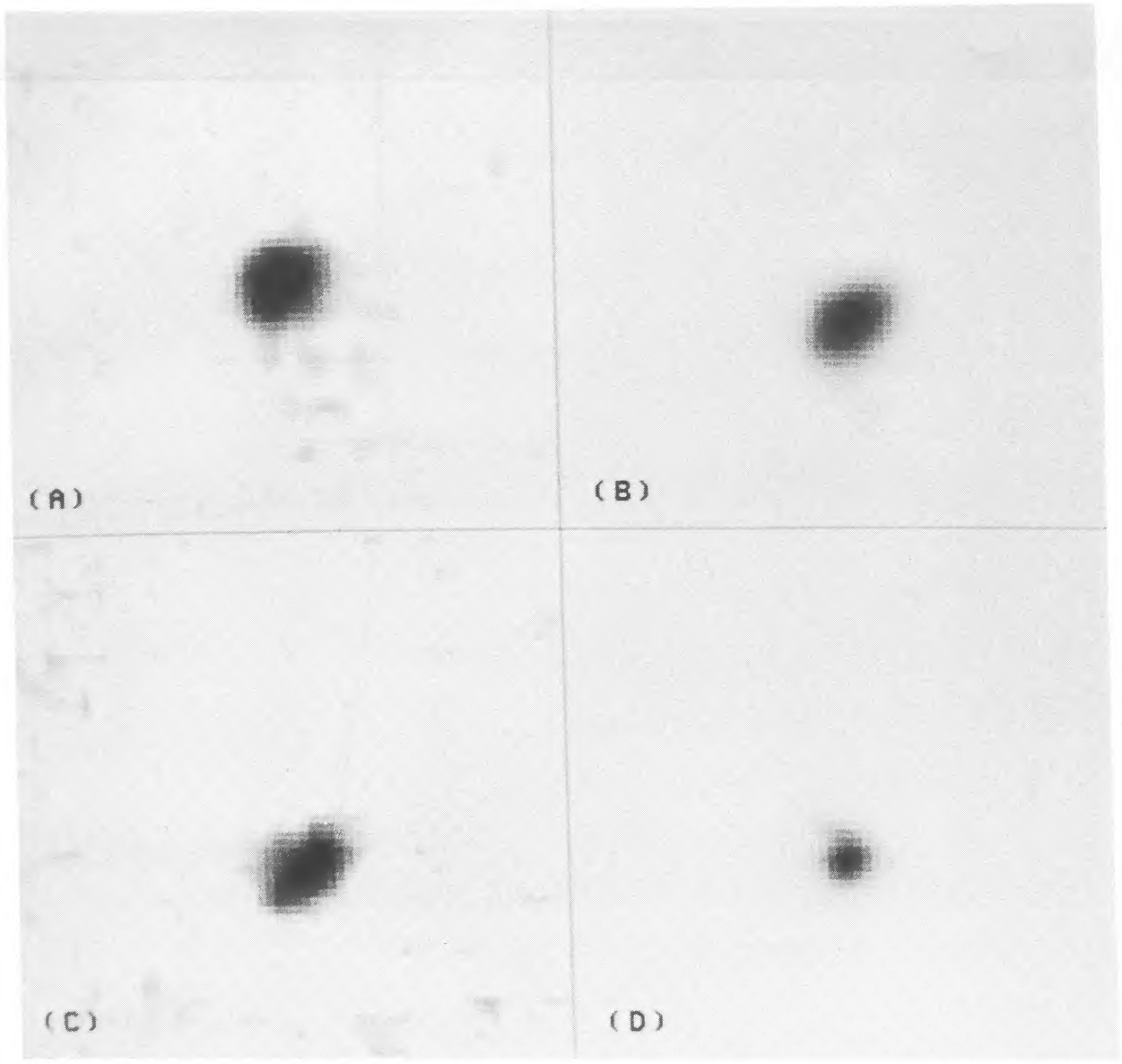

FIG. 1.—Infrared images of L 1551-IRS 5 obtained in 1984 January with the KPNO 1.3 m telescope through *H* (*top left*), *K* (*top right*), and *L'* (*bottom left*) filters. In the bottom right quadrant is the image of a point source for comparison. The images displayed are approximately 31″ on the side (see § II for details) and, as usual, north is at the top and east is to the left. The lowest levels displayed are 3% of the maximum at *H*, 0.4% at *K* for both IRS 5 and the point source, and 10% at *L'*.

(MONETI *et al. see* **327**, 871)

PLATE 9

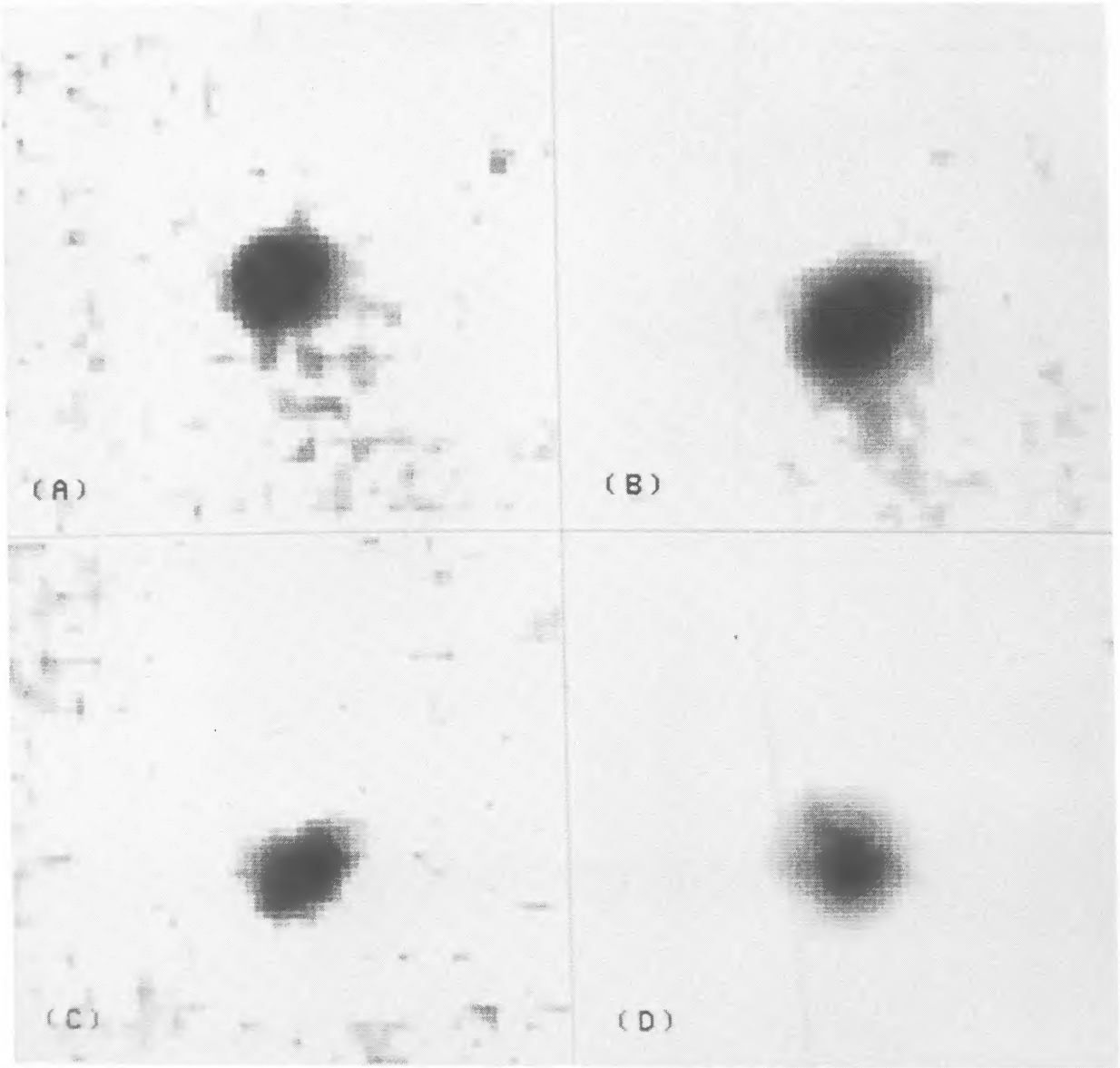

FIG. 2.—Same as Fig. 1 but scaled logarithmically in order to emphasize the regions of low surface brightness

(MONETI *et al. see* **327**, 871)

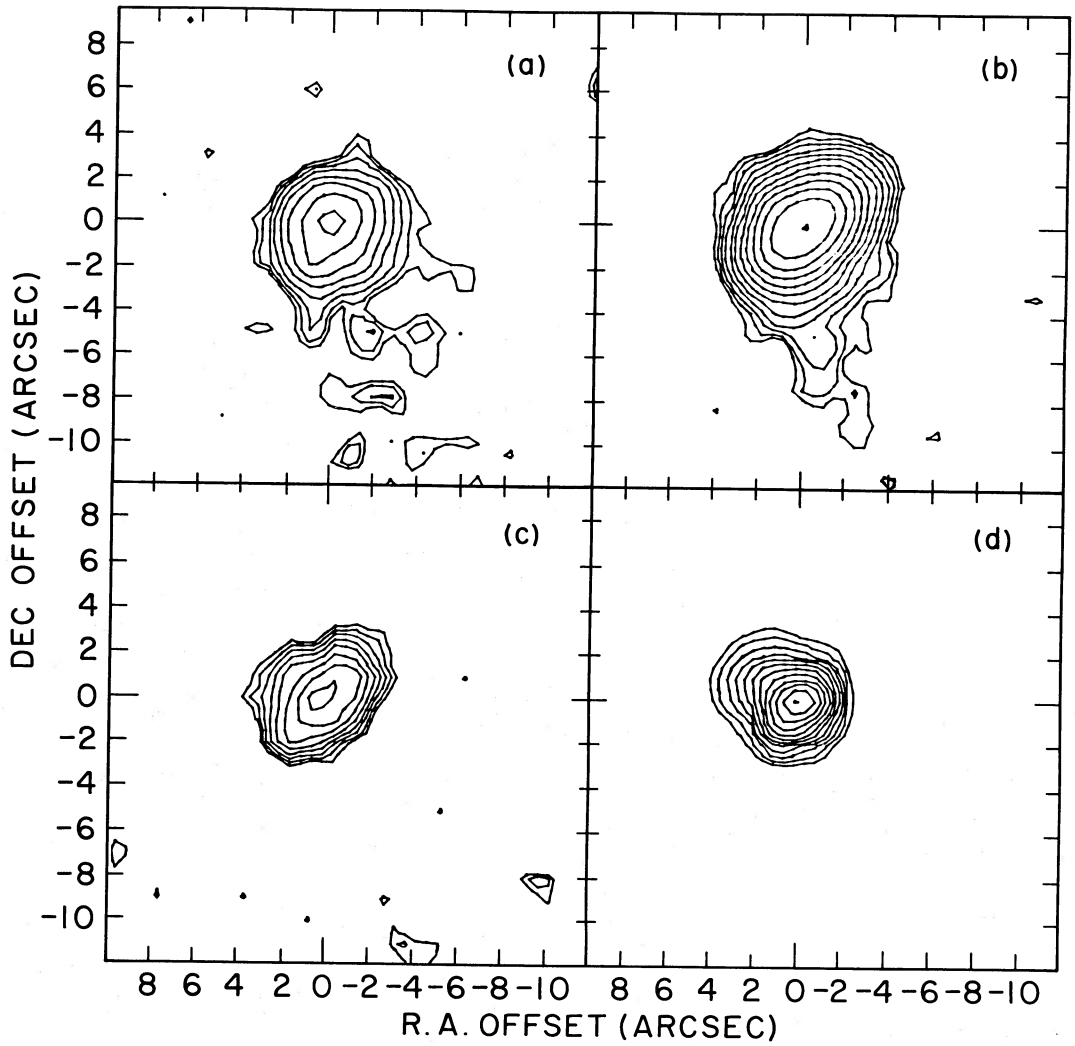

FIG. 3.—Contour maps of the IRS 5 data and of the comparison point source. The contour levels in percent of the maximum of each image are: *H* image (*a*): 6, 9, 14, 22, 33, 50, 75, 94; *K* image (*b*) and point source (*d*): 1.0, 1.6, 2.4, 3.6, 5.5, 8.3, 12.5, 19, 29, 43, 66, 99; *L'* image (*c*): 18, 23, 29, 37, 45, 57, 72, 91.

signals from all the pixels within a square region with side 8″ (our equivalent aperture) on the array were summed to give the total signal from the star. Given the total signals, standard photometric reduction techniques were applied. Experience with the array camera has shown that the results are accurate to better than ±10% or ±0.1 mag. The integrated magnitudes of IRS 5 are: $[H] = 11.4$ mag, $[K] = 9.5$ mag, and $[L'] = 6.4$ mag. There are differences of a few tenths of a magnitude between our results, those of Strom, Strom, and Vrba (1976) and those of Cohen and Schwartz (1983). These differences are probably due to the different aperture sizes used by those investigators, or they may indicate that IRS 5 is slightly variable.

III. DISCUSSION

a) The Polarization of IRS 5

i) A Bipolar Nebula?

Our results show that the direction of elongation of IRS 5 is parallel within the uncertainties to the direction of polarization. This result is contrary to what would be expected if the extended emission came from the lobes of a small bipolar nebula such as was proposed by Nagata *et al.* (1983), since in a bipolar nebula illuminated by an obscured star located between the scattering lobes (the ES model), the mean polarization will be in a direction perpendicular to the bipolar axis. We thus conclude that we are not observing a small bipolar nebula.

ii) Aligned Grains?

Aligned grains in a circumstellar envelope could polarize the light of IRS 5 as it traverses that envelope. To produce the observed polarization, the grains would have to be aligned parallel to the outflow axis. If the grains are aligned by the local magnetic field, and if the field in the envelope is parallel to the field in the rest of the L1551 cloud, then the reverse Davis-Greenstein mechanism (Jones and Spitzer 1967; Cugnon 1983) would be required. This mechanism causes alignment of the long axes of the dust grains along the magnetic field direction. However, Cugnon (1983) finds that this mechanism is very inefficient, and we conclude that it is not a likely explanation of the high observed polarization.

Alternatively, the magnetic field could be twisted in a toroidal pattern (Draper, Warren-Smith, and Scarrot 1985) in a circumstellar disk. In this case direct Davis-Greenstein grain alignment could result in grains aligned along the outflow

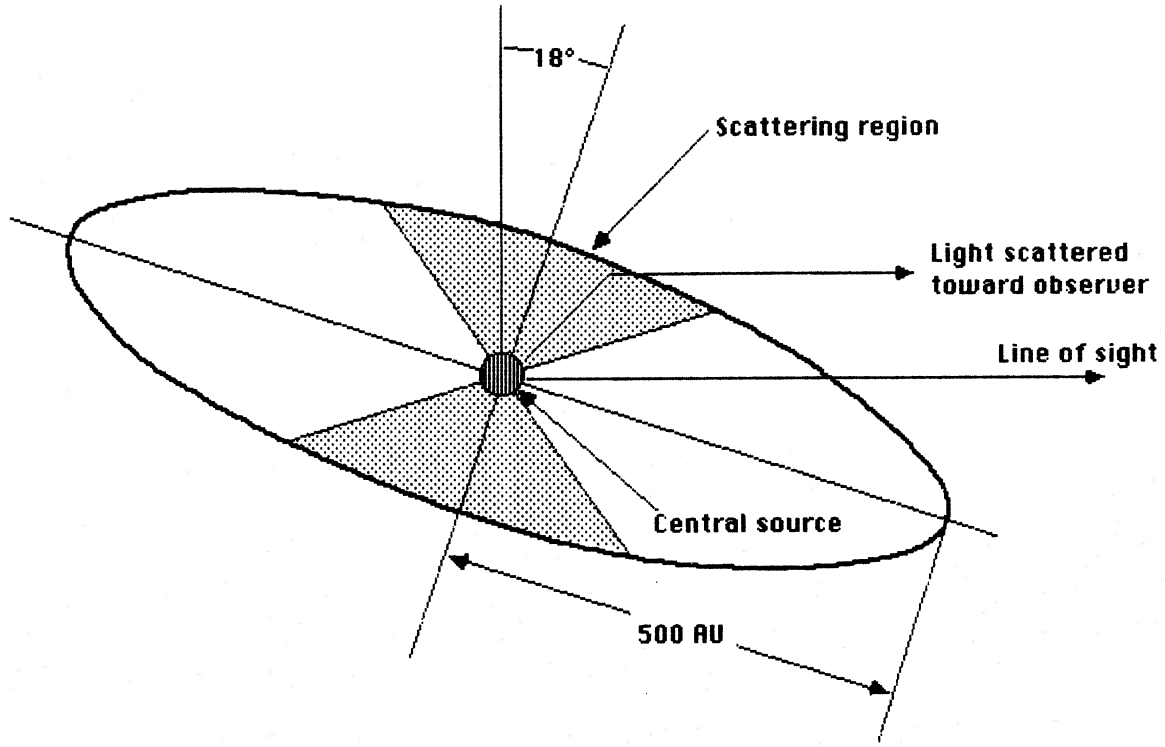

FIG. 4.—A model for the circumstellar envelope of IRS 5. The observed image is made up of light scattered from the polar region that is toward the observer. Direct light from the central star is not seen because the optical depth through that part of the envelope is too large. This model is based on Lefèvre, Daniel, and Bergeat (1983).

direction, perpendicular to the disk. Finally gas streaming (Gold 1952; Zirin 1952) in the outflow direction could provide the needed grain alignment. Since the near-infrared light is due to scattering (see § III*b*), we consider a scattering origin for the polarization as discussed in § III*c* more likely.

b) Importance of Scattering

The $H-K$ and $K-L$ gray body color temperatures determined from our data are 1000 and 800 K, respectively. The dust equilibrium temperature at a distance of 2.2×10^{15} cm (corresponding to 1″) from a 35 $L_{\odot}$ central star would be ~ 100 K for a λ^{-1} grain emissivity law, which is much lower than the observed color temperature. Therefore the observed radiation is not purely thermal dust radiation.

Thermal gas emission can be ruled out because its structure (see VLA maps) is considerably different than the near-infrared structure. In addition, extrapolating from the radio to the near-infrared, it can be seen that the thermal gas contribution to, for instance, the K band can be only 2%–3% of the total. We thus conclude that a significant amount of the observed near-infrared flux is light from the embedded star which has been scattered by dust. And if the scattering regions were asymmetrically distributed relative to the illuminating source, this could give rise to significant polarization.

c) A New Interpretation

The elliptical shape of the image can result if the source is surrounded by a flattened (oblate) circumstellar envelope of moderate optical thickness which is viewed from close to the equatorial plane (see sketch in Fig. 4). The radiative transfer problem for ellipsoidal envelopes has recently been solved using a Monte Carlo technique by Lefèvre, Daniel, and Bergeat (1983). The observed shape of an ellipsoidal envelope depends upon its true shape, its inclination to the line of sight, and its opacity. The predicted image of the envelope is made up of three components: direct light from the central star, light scattered by the envelope, and thermal dust emission from the envelope. The relative importance and the spatial distribution of each of these components will vary with wavelength and with the inclination of the envelope. Lefèvre, Daniel, and Bergeat (1983) present theoretical images of their model envelopes at 0.54 and 9 μm, which can be compared to observations taken in spectral ranges where scattering and thermal dust emission dominate, respectively. Since we have determined that scattering dominates in the K band, we will compare our K image to their 0.54 μm image. In this spectral region, most of the light comes from the region of the pole that is inclined toward the observer, where the opacity to the star is least.

Before comparing our K image to the theoretical images of Lefèvre, Daniel, and Bergeat (1983, see their Fig. 7), we note that only a qualitative comparison is possible since Lefèvre, Daniel, and Bergeat (1983) do not say to what level their contours correspond. We find that our K image is most similar to their predicted image of a 3000 K star embedded in an envelope with equatorial radius 4 times larger than the polar radius. The envelope is assumed to be filled with weakly absorptive silicate grains[4] of radius 0.1 μm, and the inclination of the envelope (defined as the angle between the polar axis and the plane of the sky) is 18°. Furthermore, since there is more low-level emission on the SW side of the IRS 5, and since,

[4] The presence of silicates in the envelope of IRS 5 is inferred from the presence of the 9.7 μm silicate feature (Cohen and Schwartz 1983).

especially at H, the observed emission drops off more steeply to the NE than to the SW, we deduce that the polar region to the SW is the one inclined toward us. This is consistent with observations of the CO outflow which show that the SW stream is blueshifted and thus is inclined toward Earth while the NE is redshifted and thus being driven into the cloud.

Another estimate of the inclination of the polar axis can be obtained if we assume that the HH objects are moving away from IRS 5 along the polar axis. For HH-29 Strom, Grasdalen, and Strom (1974) have obtained a radial velocity relative to the cloud of 45 km s^{-1}, and Cudworth and Herbig (1979) give a proper motion that corresponds to a transverse velocity of 150 km s^{-1} (the transverse velocity of the cloud, whose radial velocity is much less than 7 km s^{-1}, is expected to be less than or approximately equal to 150 km s^{-1}, and hence it should not affect our results). The inclination of the polar axis of the envelope is then given by arctan (45/150) = 17° which is essentially identical to the inclination inferred from the discussion above. Sarcander, Neckel, and Elsässer (1985) have attempted to measure the proper motion of the jet, and combining that with the jet's radial velocity they arrive at an inclination of 30°–55°. However, given the nonstellar nature of the jet, it is unclear whether the knot whose proper motion they measured is really the same object in both epochs.

Lefévre, Daniel, and Bergeat's (1983) Figure 7 shows that the major axis of the predicted image is about half the major axis of the envelope. Thus, since the observed major axis of IRS 5 is about 4″, we deduce that the size of the envelope is about twice that, or 8″. This is about 10^3 AU at the distance of the Taurus cloud, and it is about the same size as the envelope discovered by Beckwith *et al.* (1984) around R Mon. In addition, the model proposed here can qualitatively explain the polarization. Since the scattered light comes from the region of the pole that is inclined toward us, and since scattered light is polarized in a plane that is normal to the scattering plane (which contains the polar axis and the line of sight), the resulting polarization is perpendicular to the polar axis. This is consistent with the observations of Nagata, Sato, and Kobayashi (1983) and of Hodapp (1984).

Comparing the polarization in the 10 μm region to that in the near-infrared should permit one to distinguish clearly between the scattering model and the aligned grains model of polarization: given the very low scattering efficiency at 10 μm, very little polarization due to scattering would be expected there. On the other hand, cool aligned grains would provide significant polarization in the 9.7 μm silicate absorption feature which has been observed in IRS 5 (Cohen and Schwartz 1983).

d) Implications of the New Model

i) *The Density of the Envelope*

We do not see the central source directly at any wavelength, including L. This implies that $\tau(L) \gtrsim 1$, and we use this to deduce the column density of molecular hydrogen in the envelope. From Draine and Lee's (1984) Figure 8, the quantity $\lambda\tau(\text{ext})/N(\text{H}) = 6 \times 10^{-27}$ cm^3 at 3.8 μm, and from the condition that $\tau(L) \gtrsim 1$ we deduce that the number density of hydrogen molecules is greater than or approximately equal to 3.2×10^{22} cm^{-2}. If the envelope is filled with dust and gas of uniform density, and if a spherical volume is assumed for the following crude calculation, using a star to edge of envelope distance of 500 AU, we find a molecular hydrogen number density to be greater than or approximately equal to 4×10^6 cm^{-3}. This implies an envelope mass of greater than or approximately equal to 0.017 $M_\odot$.

ii) *Extinction through the Envelope*

From the above-determined lower limit on the optical depth, we can set a lower limit to the extinction through the envelope. Assuming that $A_V = 29A_{3.7\,\mu\text{m}}$ (based on the results of Draine and Lee 1984) we find that $A_V \gtrsim 33$ mag.

iii) *Mass-Loss Rate*

In the following discussion we will assume that the 18° inclination of the envelope implies a similar inclination for the axis of the CO outflow. Thus, the radial velocity of something that is moving with the flow is roughly sin 18° = 0.31 times the space velocity. Also, all radial velocities will be relative to the radial velocity of the cloud (7 km s^{-1}).

The radial velocity of the highest density region in the CO flow is 7 km s^{-1} (SLP) which implies a true velocity of $v_{\text{CO}} \approx$ 20 km s^{-1}. If the outflow has been expanding at constant velocity, then from the size of the lobes (0.5 pc) we deduce that the age of the envelope is $t_{\text{CO}} \approx 2.3 \times 10^4$ yr. From optical spectroscopy of the jet, Sarcander, Neckel, and Elsässer (1985) find that $v_{r,\text{jet}} = 150$ km s^{-1}, which implies a true jet velocity of $v_{\text{jet}} \approx 350$ km s^{-1}. To determine the mean mass-loss rate, we equate the momentum of the CO lobes, $P_{\text{CO}} = M_{\text{CO}} V_{\text{CO}}$, to the momentum of the wind, $P_{\text{wind}} = M_{\text{wind}} V_{\text{wind}} = \dot{M} t_{\text{CO}} V_{\text{wind}}$, where $\dot{M}$ is the mass-loss rate of IRS 5. Using then $V_{\text{wind}} = v_{\text{jet}}$, we obtain $\dot{M} \approx 7 \times 10^{-7}\ M_\odot$ yr^{-1}, which is comparable to the value determined by SLP who used slightly different numbers. Naturally, these results are quite sensitive to the value of the inclination angle; an uncertainty of 5° in the inclination angle produces an uncertainty of about 30% in the above results.

e) The Arc

We now return to the discussion of the arc. We confirm the interpretation of SSGCT that the arc is due to light scattered from a material (density enhancements) around IRS 5. The mean $H-K$ color temperature of the radiation from the arc, which, though highly uncertain due to the low signal level and the spatial variability at H, is of the order of 1000 K, and thus it is indicative of scattering. The arc may be part of a looplike structure similar to those observed around other young stellar objects (GL 2591, S140; Forrest and Shure 1986), and interpreted as light scattered from the edges of a bubble or cavity evacuated by the stellar wind of the illuminating star. Further deeper observations will be needed to confirm this hypothesis.

IV. CONCLUSION

We have presented new, high spatial resolution near-infrared images of the young star L1551-IRS 5. These images clearly show that the source is extended, and that it is elongated in a direction perpendicular to the bipolar CO outflow. The source does not mainly consist of the bipolar scattering lobes that were expected on the basis of the large polarization, and thus the polarization is not due to the Elsässer and Staude mechanism.

A new model has been proposed, based on theoretical images of Lefévre, Daniel, and Bergeat (1983), in which the source consists of a central star which is surrounded by a flattened envelope of moderate optical thickness (in the near-infrared), and which is oriented with its polar axis at an angle of ~18° to the plane of the sky. At the near-infrared wavelengths we do not see directly the central star, but we see light

from the central star that is scattered by dust grains in one of the polar regions of the envelope. We also deduce that the envelope is some 1000 AU in diameter and that its mean density of molecular hydrogen, assumed to be uniform, is greater than or approximately equal to 4×10^6 cm^{-3}. Furthermore, this geometry explains naturally the direction of the observed infrared polarization.

Finally, the inferred inclination angle of the envelope is supported by the space velocity of HH-29, one of the HH objects in the blueshifted CO lobe, whose inclination is also at about 20°.

We wish to thank the Kitt Peak staff, especially Dick Joyce, Ron Probst, and Chuck Mahaffey for their help throughout the observing run. Development of the array camera at the University of Rochester was supported by NASA Ames grant NAG 2-117 and by the Office of Naval Research grant CNA SUB N00014-76-C-0001.

REFERENCES

Becklin, E. E. Neugebauer, G., and Wynn-Williams, C. G. 1973, *Ap. J. (Letters)*, **182**, L7.
Beckwith, S., Zuckerman, B., Skrutskie, M. F., and Dyck, H. M. 1984, *Ap. J.*, **287**, 793.
Cohen, M., and Schwartz, R. D. 1983, *Ap. J.*, **265**, 877.
Cudworth, K. M., and Herbig, G. 1979, *A.J.*, **84**, 548.
Cugnon, P. 1983, *Astr. Ap.*, **120**, 156.
Davidson, J. A., and Jaffe, D. T. 1984, *Ap. J. (Letters)*, **277**, L13.
Draine, B. T., and Lee, H. M. 1984, *Ap. J.*, **285**, 89.
Draper, P. W., Warren-Smith, R. F., and Scarrot, S. M. 1985, *M.N.R.A.S.*, **216**, 7P.
Elias, J. H. 1978, *Ap. J.*, **224**, 857.
Elsässer, H., and Staude, H. J. 1978, *Astr. Ap.*, **70**, L3 (ES).
Emerson, J. P., Harris, S., Jennings, R. E., Beichman, C. H., Baud, B., Beintema, D. A., Marsden, P. L., and Wesselius, P. R. 1984, *Ap. J. (Letters)*, **278**, L49.
Forrest, W. J., Moneti, A., Woodward, C. E., Pipher, J. L., and Hoffman, A. 1985, *Pub. A.S.P.*, **97**, 183.
Forrest, W. J., and Shure, M. 1986, *Ap. J. (Letters)*, **311**, L81.
Gold, T. 1952, *M.N.R.A.S.*, **112**, 215.
Hodapp, K. 1984, Ph.D. dissertation, Ruprecht-Karls-Universität, Heidelberg.
Jones, R. V., and Spitzer, L., Jr. 1967, *Ap. J.*, **147**, 943.
Königl, A. 1982, *Ap. J.*, **261**, 115.
Lefévre, J., Daniel, J.-Y., and Bergeat, J. 1983, *Astr. Ap.*, **121**, 51.
Mirabel, I. F., Rodríguez, L. F., Canto, J., and Arnal, E. M. 1985, *Ap. J. (Letters)*, **294**, L39.
Moneti, A. 1984, Ph.D. dissertation, University of Rochester.
Moneti, A., Pipher, J. P., Forrest, W. J., and Woodward, C. E. 1986, in *Light on Dark Matter*, ed. F. P. Israel (Dordrecht: Reidel), p. 315.
Moriarty-Schieven, G. H., Snell, R. L., Strom, S. E., and Grasdalen, G. L. 1987, *Ap. J. (Letters)*, **317**, L95.
Mundt, R., and Fried, J. 1983, *Ap. J. (Letters)*, **274**, L83.
Nagata, T., Sato, S., and Kobayashi, Y. 1983, *Astr. Ap.*, **119**, L1.
Nagata, T., Yamashita, T., Sato, S., Suzuki, H., Hough, J. H., Garden, R., and Gatley, I. 1986, *M.N.R.A.S.*, **223**, 7P.
Rodríguez, L. F., Canto, J., Torrelles, J. M., and Ho, P. T. P. 1986, *Ap. J. (Letters)*, **301**, L25.
Sarcander, M., Neckel, T., and Elsässer, H. 1985, *Ap. J. (Letters)*, **288**, L51.
Snell, R. L., Bally, J., Strom, S. E., and Strom, K. M. 1985, *Ap. J.*, **290**, 587.
Snell, R. L., and Schloerb, F. P. 1985, *Ap. J.*, **295**, 490.
Snell, R. L., Loren, R. B., and Plambeck, R. L. 1980, *Ap. J. (Letters)*, **239**, L17 (SLP).
Strom, S. E., Strom, K. M., Grasdalen, G. L., Capps, R. W., and Thompson, D. 1985, *A.J.*, **90**, 2575 (SSCGT).
Strom, K. M., Strom, S. E., and Vrba, F. J. 1976, *Astr. Ap.*, **81**, 320.
Strom, S. E., Grasdalen, G. L., and Strom, K. M. 1974, *Ap. J.*, **191**, 111.
Vrba, F. J., Strom, S. E., and Strom, K. M. 1976, *A.J.*, **81**, 958.
Werner, M. W., and Salpeter, E. E. 1969, *M.N.R.A.S.*, **145**, 245.
Zirin, H. 1952, *Harvard Obs. Bull.* No. 921, 26.

WILLIAM J. FORREST and JUDITH L. PIPHER: Department of Physics and Astronomy, University of Rochester, Rochester, NY 14627

ANDREA MONETI: European Southern Observatory, Karl-Schwarzschild-Strasse 2, D-8046 Garching bei München, Federal Republic of Germany

CHARLES E. WOODWARD: Department of Physics and Astronomy, University of Wyoming, P.O. Box 3905, Laramie, WY 82071